Electronic Supplementary Information

Green Synthesis of Zr-Based Metal-Organic Framework Hydrogel Composites and Their Enhanced Adsorptive Properties

Shirell E. Klein,[a] Joshua D. Sosa,[a] Alexander C. Castonguay,[b] Willmer I. Flores,[a] Lauren D. Zarzar,[bcd] and Yangyang Liu[a*]*

[a]Department of Chemistry and Biochemistry, California State University Los Angeles, 5151 State University Dr, Los Angeles, CA 90032, United States

[b]Department of Chemistry, [c]Department of Materials Science and Engineering, Pennsylvania State University, University Park, PA 16802, United States

[d]Materials Research Institute, Pennsylvania State University, University Park, PA 16802, United States

yliu114@calstatela.edu

ldz4@psu.edu

Table of content

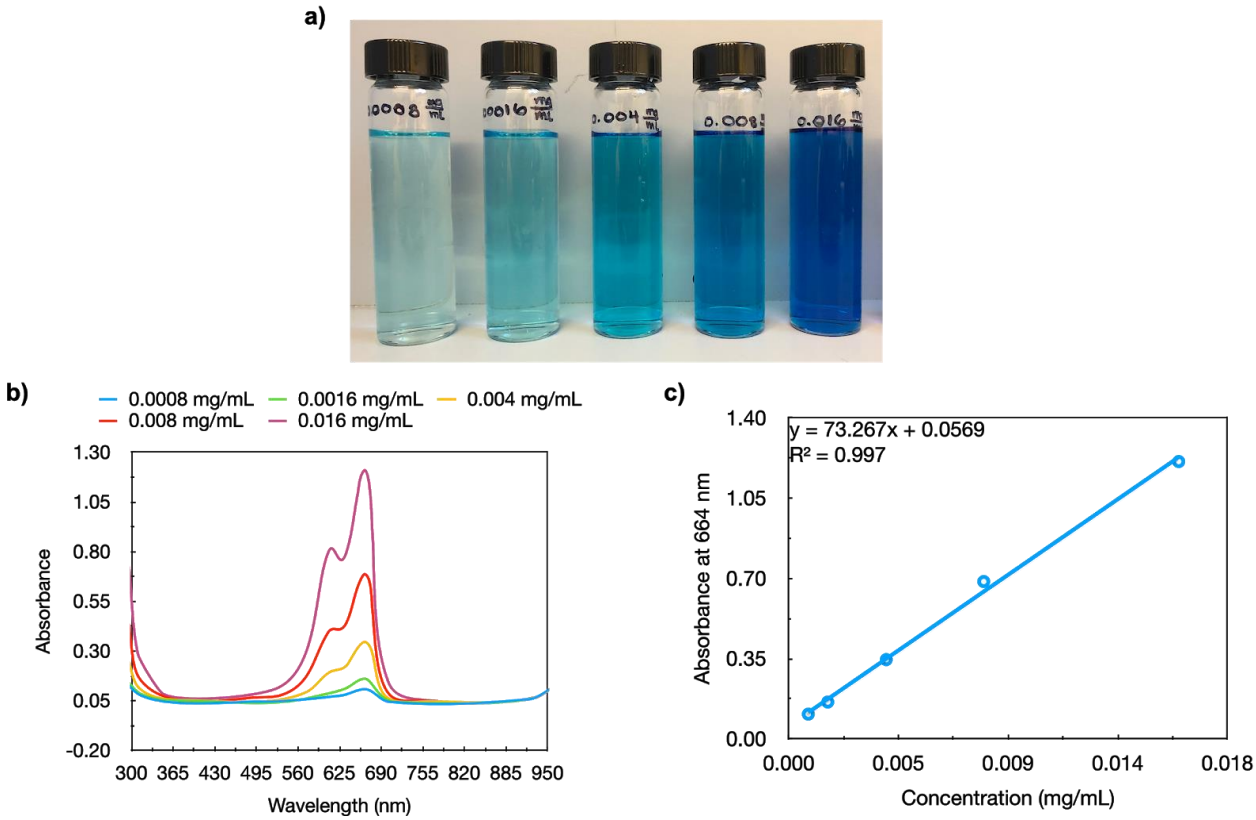

Figure S1. Methylene blue absorbance calibration. (a) 0.0008, 0.0016, 0.004, 0.008, 0.016, and 0.04 mg/mL methylene blue solutions (from left to right), (b) measured absorbance for each methylene blue solution, and (c) calibration curve for MB concentration based on absorbance at 664 nm ($R^2 = 0.997$).

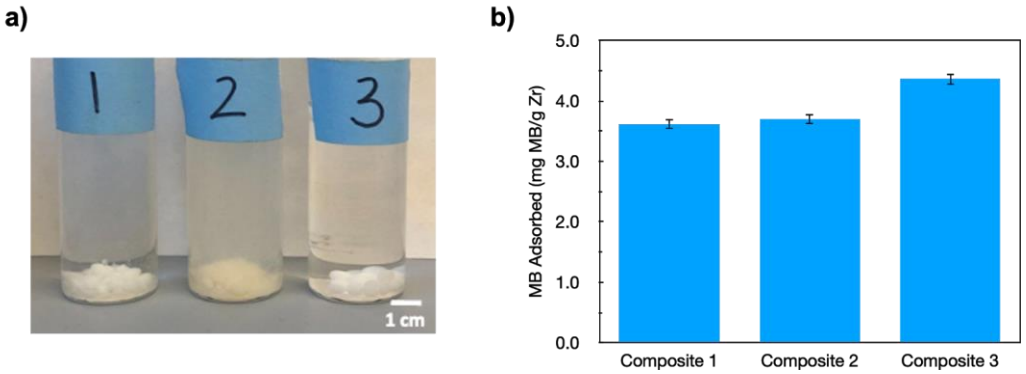

Figure S2. Stability and dye adsorption comparison of composites 1, 2, and 3. (a) Visual comparison shows the increased structural stability of composite 3 directly after synthesis. Composite 1 and 2 gels fell apart during solvothermal linker incorporation. (b) Relative MB adsorption by the composites (performed in duplicate and shown as average with standard deviation for error). All three composites showed relatively high MB adsorption, with the highest adsorption by composite 3. This, in addition to the increased structural stability, resulted in identification of composite 3 as the best hybrid for further testing.

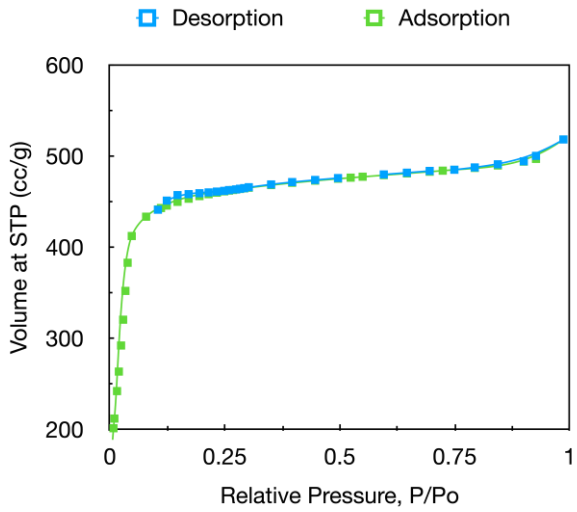

Figure S3. Nitrogen isotherm of MOF-808 at 77K (BET surface area = 1941.454 m^2/g).

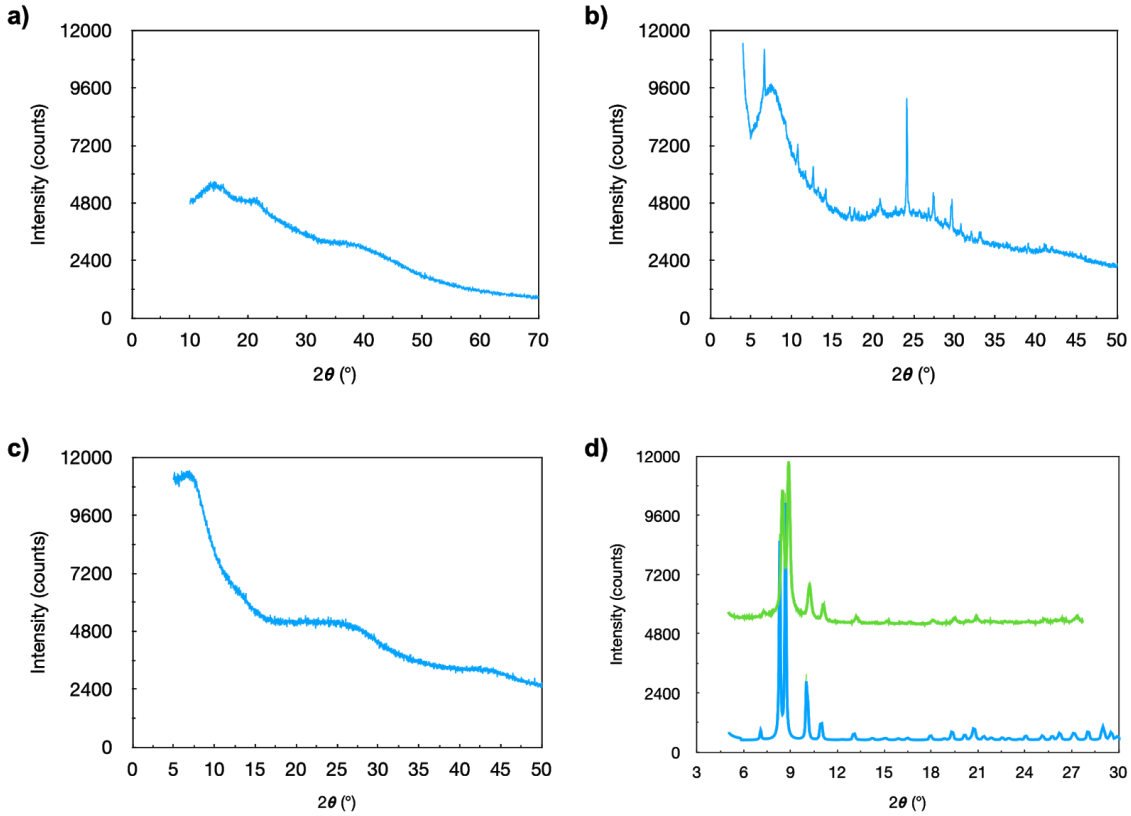

Figure S4. PXRD of (a) heat dried Zr-Alg, (b) heat dried composite 3, (c) supercritical CO_2 dried composite 3, and (d) simulated MOF-808 pattern (blue) compared to synthesized MOF-808 (green).

PXRD patterns observed in the heat dried composite 3 align with PXRD patterns for the trimesic acid linker, indicating the dissociation of trimesic acid from the composite due to decomposition. On the other hand, the supercritical CO_2 dried composite 3 showed amorphous character with no peaks arising from ligand (trimesic acid) dissociation. PXRD data suggest that composite 3 structure collapsed under heat dry condition, but supercritical CO_2 drying can remove the solvent in the composite while maintaining its porous structure.

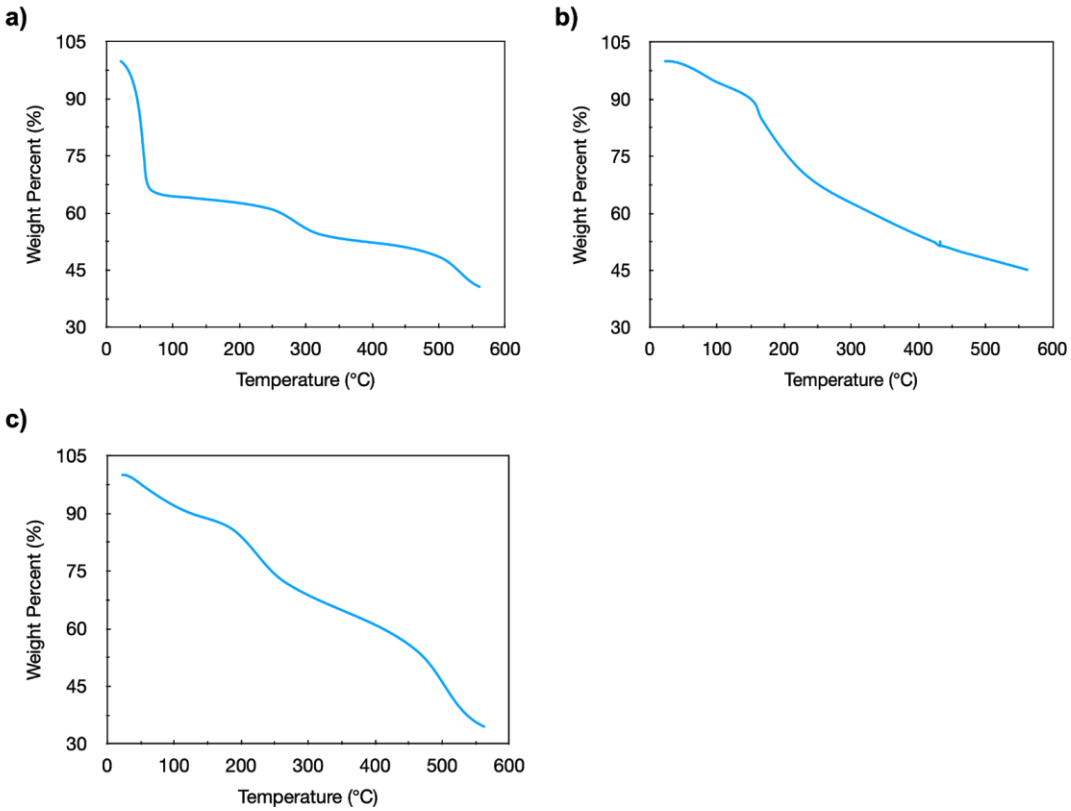

Figure S5. TGA of (a) MOF-808, and supercritical CO_2 dried (b) Zr-Alg hydrogels and (c) composite 3. Both MOF-808 and composite 3 displayed a step in weight % corresponding to the decomposition of trimesic acid (starting ~500 K), which was not observed for the Zr-Alg hydrogel. This helped to confirm the successful incorporation of trimesic acid into composite 3.

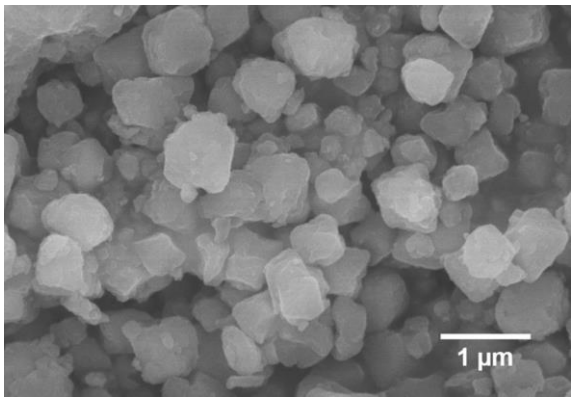

Figure S6. SEM characterization of MOF-808 particles. Particle sizes were observed between 200-700 nm.

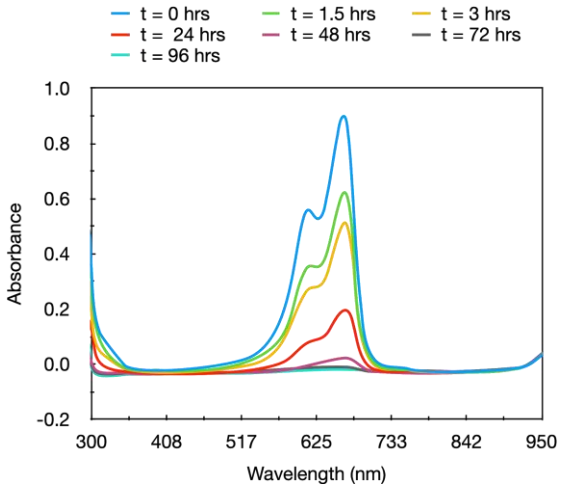

Figure S7. Determination of time needed for complete encapsulation of MB dye by composite 3. Composite 3 samples were placed in solutions of 0.0096 mg/mL MB and allowed to load the dye for 1.5, 3, 24, 48, 72, and 96 hours before measuring the remaining MB in the supernatant by UV-vis. Minimal change was observed after 72 hours.

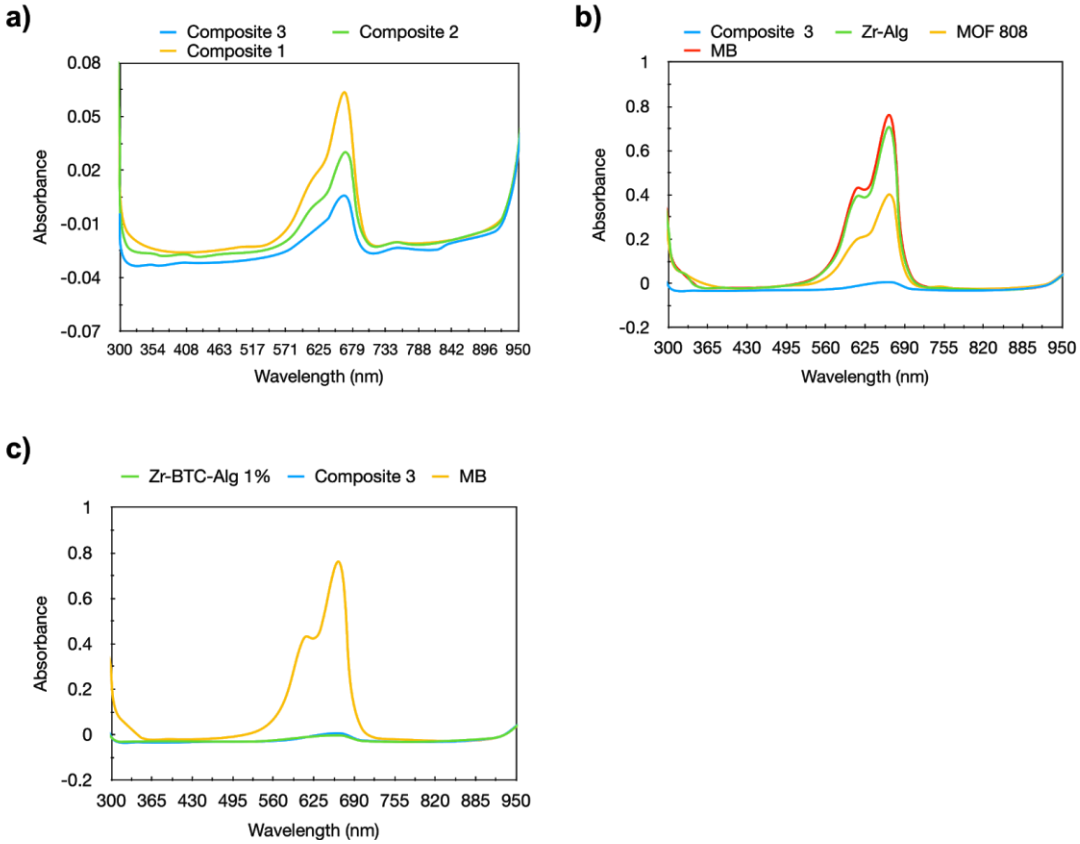

Figure S8. UV-vis of supernatant following dye encapsulation show relative loading of methylene blue (MB) by (a) composite 3 (Zr-Alg 2%) compared with previous literature hybrids (composite 1 and composite 2), (b) composite 3 compared with MOF-808 and Zr-Alg hydrogels, and (c) composite 3 compared with decreased alginate concentration hydrogels. It was assumed that all Zr^{4+} used in the synthesis was incorporated into the gels. This assumption was based on the equal dye adsorption in samples with varying alginate concentrations.

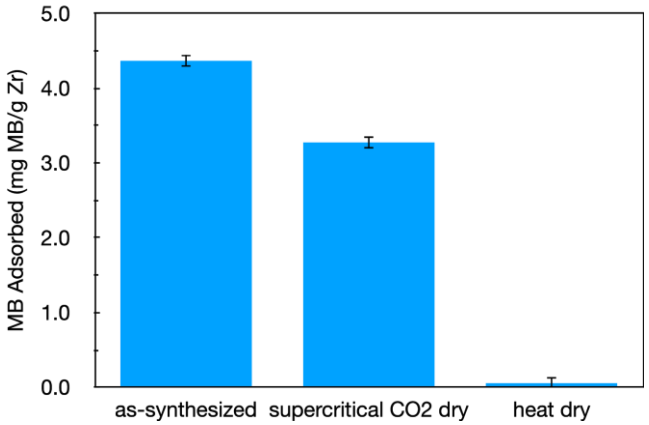

Figure S9. Comparison of supercritical CO_2 drying and heat drying methods for composite 3 (performed in duplicate and shown as average with standard deviation for error). After activation of composite 3 by supercritical CO_2 drying, a minimal decrease in adsorption was observed (the composite retained 75% of the original loading capacity), whereas the heat dried sample showed significant decrease of MB adsorption. Given the probable collapse of large voids within composite 3 upon heat drying, supercritical CO_2 drying was determined to be a preferable method for activation.

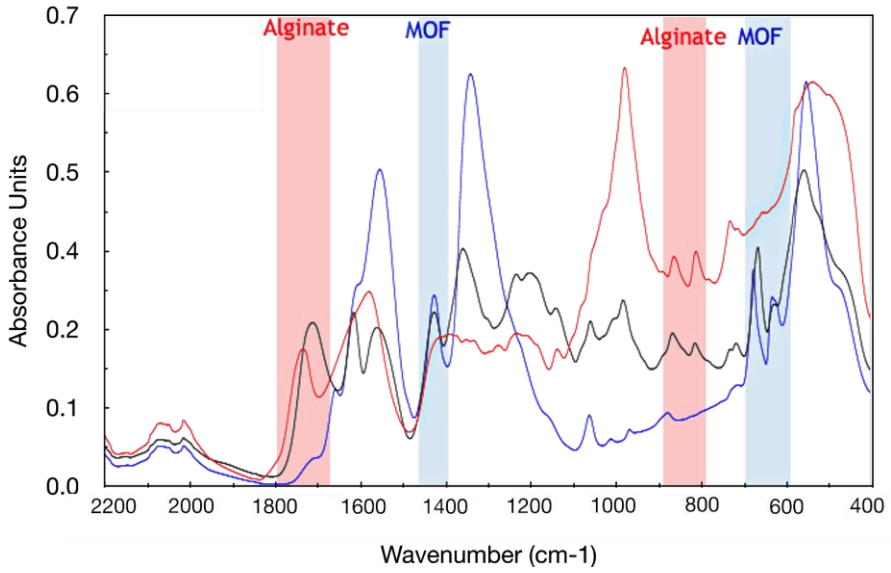

Figure S10. FTIR of MOF-808 (blue), dried sodium alginate (red), and composite 3 (black). Red shifting in the alginate CO peak (1723 cm^{-1}) is indicative of new interactions at these sites in composite 3, presumably resultant from ionic bonding between the alginate carboxylate groups and Zr^{4+} ions.

Additional red shifting in the MOF Zr-O peak (755 cm^{-1}) signifies a change in ligand environment, indicating zirconium bonding to both the alginate and trimesic acid linker in composite 3. Characteristic peak alignment or red-shifting is highlighted in blue for comparison of composite 3 with MOF-808 and red for comparison of composite 3 with dried alginate.

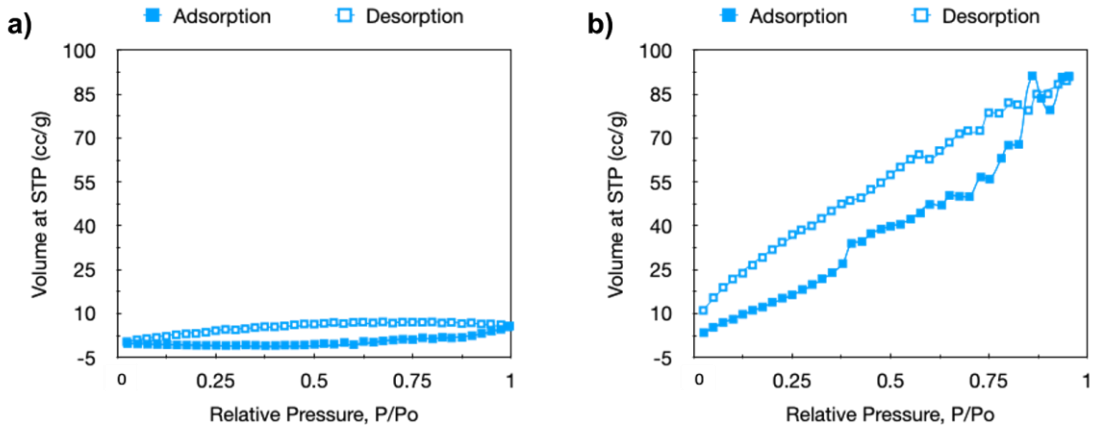

Figure S11. Nitrogen isotherms of supercritical CO_2 dried (a) Zr-Alg hydrogel (BET surface area = 0.600 m^2/g) and (b) composite 3 (BET surface area = 80.076 m^2/g) at 77 K.

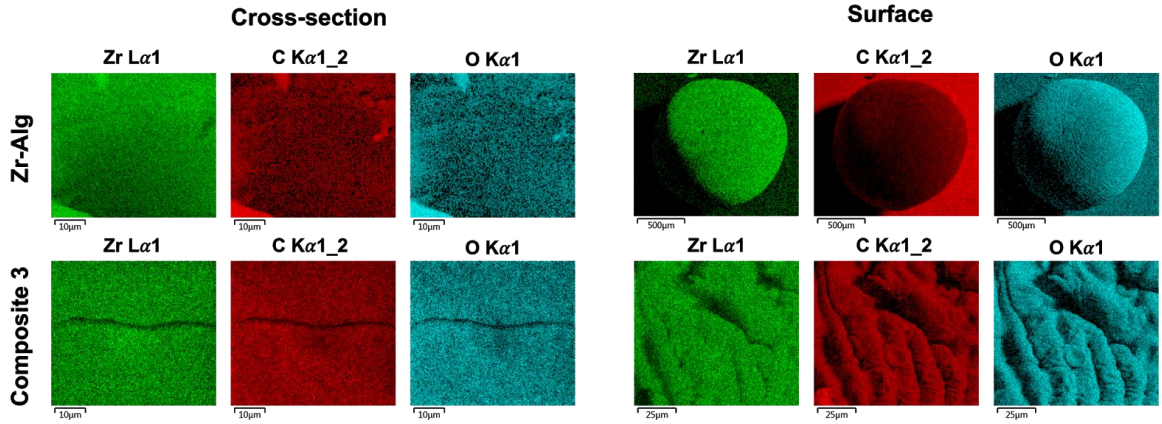

Figure S12. Energy-dispersive X-ray spectroscopy (EDS) of Zr-Alg hydrogel (top row) and composite 3 (bottom row). All images show even distributions of zirconium, carbon, and oxygen, suggesting uniform composition.

Table S1. Tabulated methylene blue adsorption capacities of composite **3**, Zr-Alg hydrogel, and MOF-808 at initial MB concentration of 30.014 uM with varied solution pH and ionic strength (all samples performed in triplicate, shown as average with standard deviation for error). PC was calculated as mg MB adsorbed per g Zr partitioned from uM MB remaining in the supernatant.

Sample	Final Concentration (uM MB)	Ionic Strength	pH	MB Adsorbed (mg MB/g Zr)	PC (mg/g/uM)
Composite 3	12.309	0	13.0	3.735 ± 0.157	0.097 ± 0.004
Composite 3	10.580	0	12.7	3.806 ± 0.160	0.115 ± 0.005
Composite 3	6.963	0	12.0	4.028 ± 0.169	0.185 ± 0.008
Composite 3	9.279	0	8.5	4.334 ± 0.249	0.149 ± 0.009
Composite 3	8.101	0	7.0	4.361 ± 0.183	0.172 ± 0.007
Composite 3	9.163	0	5.5	4.343 ± 0.072	0.152 ± 0.003
Composite 3	11.262	0	2.0	3.425 ± 0.072	0.097 ± 0.002
Composite 3	13.219	0	1.3	2.704 ± 0.057	0.065 ± 0.001
Composite 3	13.173	0	1.0	2.429 ± 0.051	0.059 ± 0.001
Composite 3	8.874	0.2	7.0	4.966 ± 0.372	0.179 ± 0.013
Composite 3	9.472	1.0	7.0	4.822 ± 0.489	0.163 ± 0.017
Zr-Alg	11.968	0	13.0	0.743 ± 0.150	0.020 ± 0.004
Zr-Alg	10.694	0	12.7	0.654 ± 0.132	0.020 ± 0.004
Zr-Alg	4.506	0	12.0	0.489 ± 0.099	0.035 ± 0.007
Zr-Alg	66.010	0	8.5	0.339 ± 0.038	0.002 ± 0.001
Zr-Alg	20.726	0	7.0	0.502 ± 0.142	0.008 ± 0.002

Zr-Alg	65.907	0	5.5	0.315 ± 0.051	0.002 ± 0.001
Zr-Alg	20.453	0	2.0	0.491 ± 0.099	0.008 ± 0.002
Zr-Alg	19.634	0	1.3	1.298 ± 0.262	0.021 ± 0.004
Zr-Alg	18.815	0	1.0	0.749 ± 0.151	0.013 ± 0.003
Zr-Alg	30.621	0.2	7.0	0.254 ± 0.150	0.003 ± 0.002
Zr-Alg	27.360	1.0	7.0	0.810 ± 0.342	0.009 ± 0004
MOF-808	4.141	0	13.0	4.341 ± 0.340	0.335 ± 0.026
MOF-808	13.864	0	12.7	1.850 ± 0.169	0.011 ± 0.001
MOF-808	18.693	0	12.0	0.614 ± 0.076	0.011 ± 0.001
MOF-808	19.750	0	8.5	0.343 ± 0.168	0.006 ± 0.003
MOF-808	18.465	0	7.0	0.672 ± 0.059	0.012 ± 0.001
MOF-808	20.572	0	5.5	0.133 ± 0.067	0.002 ± 0.001
MOF-808	18.489	0	2.0	0.665 ± 0.073	0.012 ± 0.001
MOF-808	18.094	0	1.3	0.767 ± 0.069	0.014 ± 0.001
MOF-808	17.909	0	1.0	0.814 ± 0.077	0.015 ± 0.001
MOF-808	13.451	0.2	7.0	1.956 ± 0.306	0.047 ± 0.007
MOF-808	2.937	1.0	7.0	4.649 ± 0.126	0.506 ± 0.014